HHS Public Access

Author manuscript

J Bone Miner Res. Author manuscript; available in PMC 2017 May 01.

Published in final edited form as:

J Bone Miner Res. 2016 May ; 31(5): 949–963. doi:10.1002/jbmr.2757.

Hydrogen Sulfide Is a Novel Regulator of Bone Formation Implicated in the Bone Loss Induced by Estrogen Deficiency

Francesco Grassi[1,*], **Abdul Malik Tyagi**[2,*], **John W Calvert**[3], **Laura Gambari**[4], **Lindsey D Walker**[2], **Mingcan Yu**[2], **Jerid Robinson**[2], **Jau-Yi Li**[2], **Gina Lisignoli**[4], **Chiara Vaccaro**[2], **Jonathan Adams**[2], and **Roberto Pacifici**[2,5]

[1]Laboratorio Ramses Istituto Ortopedico Rizzoli, Bologna, Italy

[2]Division of Endocrinology, Metabolism, and Lipids, Department of Medicine, Emory University, Atlanta, GA, USA

[3]Division of Cardiothoracic Surgery, Department of Surgery, Emory University, Atlanta, GA, USA

[4]Laboratorio di Immunoreumatologia e Rigenerazione Tissutale, Istituto Ortopedico Rizzoli, Bologna, Italy

[5]Immunology and Molecular Pathogenesis Program, Emory University, Atlanta, GA, USA

Abstract

Hydrogen sulfide (H_2S) is a gasotransmitter known to regulate bone formation and bone mass in unperturbed mice. However, it is presently unknown whether H_2S plays a role in pathologic bone loss. Here we show that ovariectomy (ovx), a model of postmenopausal bone loss, decreases serum H_2S levels and the bone marrow (BM) levels of two key H_2S-generating enzymes, cystathione β-synthase (CBS) and cystathione γ-lyase (CSE). Treatment with the H_2S-donor GYY4137 (GYY) normalizes serum H_2S in ovx mice, increases bone formation, and completely prevents the loss of trabecular bone induced by ovx. Mechanistic studies revealed that GYY increases murine osteoblastogenesis by activating Wnt signaling through increased production of the Wnt ligands Wnt16, Wnt2b, Wnt6, and Wnt10b in the BM. Moreover, in vitro treatment with 17β-estradiol upregulates the expression of CBS and CSE in human BM stromal cells (hSCs), whereas an H_2S-releasing drug induces osteogenic differentiation of hSCs. In summary, regulation of H_2S levels is a novel mechanism by which estrogen stimulates osteoblastogenesis and bone formation in mice and human cells. Blunted production of H_2S contributes to ovx-induced bone loss in mice by limiting the compensatory increase in bone formation elicited by ovx. Restoration of H_2S levels is a potential novel therapeutic approach for postmenopausal osteoporosis.

Address correspondence to: Roberto Pacifici, MD, Division of Endocrinology, Metabolism, and Lipids, Emory University School of Medicine, 101 Woodruff Circle, Room 1309, Atlanta, GA 30322, USA. roberto.pacifici@emory.edu.

*FG and AMT contributed equally to this work.

Authors' roles: FG, AMT, and RP designed this study. FG, AMT, LG, GL, and JC carried out the experiments. Data collection was done by CV, LG, JR, JA, MY, JL, and LW. FG, RP, JC, and AMT conducted the data analysis. FG, LG, RP, and AMT interpreted the data. The manuscript was drafted and revised by RP, FG, and AMT.

Disclosures

All authors state that they have no conflicts of interest.

Additional Supporting Information may be found in the online version of this article.

Keywords

HYDROGEN SULFIDE; OSTEOPOROSIS; OVARIECTOMY; BONE LOSS; WNT SIGNALING

Introduction

Postmenopausal osteoporosis is a common skeletal disease leading to fracture and disability that stems from the cessation of ovarian function at menopause and from genetic and nongenetic factors that heighten the impact of estrogen deficiency on the skeleton.[1,2] Fractures owing to osteoporosis have devastating consequences, particularly in the elderly. Vertebral fractures are a source of significant pain and crippling, whereas hip fractures lead to mortality rates of 24% to 30% in the first year alone. Furthermore, almost 50% of survivors suffer permanent disability.[3–6]

Declining estrogen levels result in a potent stimulation of bone resorption and, to a lesser extent, bone formation, leading to a period of rapid bone loss.[7] This initial phase is followed by a slower but more prolonged period of bone loss that affects mostly the cortical compartment of the skeleton. The acute effects of menopause are modeled by ovariectomy (ovx) that, like natural menopause, stimulates bone resorption by increasing osteoclast formation[8,9] and life span.[10–12]

The net bone loss caused by ovx is limited by an increase in bone formation resulting from stimulated osteoblast formation.[13] This compensation is fueled by an expansion of the pool of stromal cells (SCs), increased commitment of such pluripotent precursors toward the osteoblastic lineage,[13] and enhanced proliferation of early osteoblast precursors.[14] Subsequent escalations in osteoblast apoptosis,[15,16] extensions of osteoclast life span,[10,11] increased oxidative stress,[17] and increased secretion of cytokines, which suppress bone formation such as IL-7 and TNFα,[8] contribute to the explanation of why bone formation does not increase as much as resorption after ovx. However, the mechanism that prevents bone formation from increasing sufficiently to offset bone resorption is still largely unknown.

Hydrogen sulfide (H_2S) is a gasotransmitter released endogenously by mammalian cells. H_2S is enzymatically generated in several tissues, including the vasculature, kidney, heart, brain, nervous system, lung, upper and lower GI tract,[18] and bone.[19] H_2S production is mainly controlled by two pyridoxal-5′-phosphate-dependent enzymes, cystathione-β-synthase (CBS) and cystathione-γ-lyase (CSE).[20] H_2S acts as a physiological messenger molecule in organs and tissues.[20] First identified as a neuromodulator,[21] H_2S was found to be a potent vasodilator[22] to protect cells against oxidative stress by restoring glutathione levels[23] and by inducing the nuclear translocation of Nrf2, the transcription factor that regulates a number of antioxidant genes.[24,25] Moreover, H_2S protects against inflammation by inhibiting lymphocyte infiltration in tissues[26] and impairing T-cell proliferation.[27] H_2S production in cells was proposed as the unifying mechanism by which different calorie-restriction regimens trigger increased life span in diverse organisms, suggesting a key role of H_2S in the protection against aging-associated diseases.[28] Attesting to relevance, H_2S

levels in humans decline after the age of 50 years,[29] and low levels of plasmatic H_2S are associated with several diseases, such as diabetes,[30] atherosclerotic disease,[31] and hypertension.[32,33]

H_2S is also relevant for the acquisition and preservation of bone mass because it controls SC function by regulating Ca^{2+} influx through Ca^{2+} channels.[19] H_2S deficiency impairs the osteogenic differentiation of SCs.[19] Accordingly, CBS-deficient mice display an osteopenic phenotype[19,34] reminiscent of the human inherited genetic disorder hyperhomocysteinemia, which stems from mutations in the CBS gene. Severe, premature osteoporosis is a feature of this condition.[35] The capacity of H_2S to regulate osteoblastogenesis, its production by SCs, and the decrease in H_2S levels in aging prompted us to investigate whether estrogen deficiency impairs the endogenous synthesis of H_2S and the role of H_2S in ovx-induced bone loss. We report that estrogen regulates the production of H_2S in the SCs via a direct regulation of CBS and CSE; we also show that pharmacological restoration of normal levels of H_2S prevents ovx-induced bone loss by enhancing bone formation.

Materials and Methods

Reagents and chemicals

GYY was purchased from Cayman Chemicals (Ann Arbor, MI, USA). All fine chemicals including NaHS, DMSO, and primers were purchased from Sigma-Aldrich (St. Louis, MO, USA). P1NP and CTX ELISA kit were purchased from Immunodiagnostic Systems Ltd. (Boldon, UK).

Human bone marrow (BM) cells

All studies based on human cells were approved by the Ethical Committee of Rizzoli Orthopedic Institute. hSCs were obtained as previously described.[36] Briefly, hSCs were obtained from BM aspirate during hip-replacement surgery of 6 posttraumatic patients. The cells were washed twice and suspended in α-MEM 15% fetal bovine serum (FBS; Lonza, Basel, Switzerland), counted, and plated in flask. After 1 week, nonadherent cells were removed and the adherent h-SCs expanded in vitro. hSCs were used at passage 3 in culture. hSCs were stimulated with 17β-Estradiol (Sigma, Milan, Italy) at concentrations ranging from 10^{-8} to 10^{-9} M for 24 hours. Cells and unstimulated controls were then harvested and lysed for subsequent mRNA expression analyses of CBS and CSE genes.

In vivo murine studies

All animal procedures were approved by the Institutional Animal Care and Use Committee of Emory University. Adult female C57BL/6 mice (9 to 10 weeks old) were used for the study. All mice were housed at 25°C in 12-hour light/dark cycles. Normal chow diet and water were provided *ad libitum.* For the first set of experiments, 10 mice per group were taken. The mice were divided into four groups: sham-operated (ovary intact) mice treated with either GYY or vehicle and ovariectomized (ovx) mice treated with either GYY or vehicle. The treatment was given as intraperitoneal (ip) injections of GYY/vehicle every other day at 1 mg/mouse for 4 weeks after ovx. For therapeutic study, 10-week-old female

mice were divided into the same four groups as in the first experiment. After performing ovx surgery, we left these mice for 4 weeks without treatment. Ovx mice developed osteopenia in these 4 weeks. After 4 weeks, we treated mice either with GYY or vehicle for 4 weeks with the same regime as we treated in the first experiment. Animals were euthanized after 4 weeks of treatment. At death, uterus was carefully dissected and weighed in each mouse to assess for estrogen agonistic activity.

Mineralization assay

For in vitro mineralization, hSCs were cultured in α-MEM 20% FBS supplemented with 100 mM ascorbic acid, 2 mM α-glycerophosphate, and 100 nM dexamethasone (all from Sigma, Milan, Italy), with or without NaHS for 21 days with a medium change every 48 hours. At the end of the experiment, cells were washed with vehicle and fixed with paraformaldehyde (4%) in vehicle for 15 minutes and stained with Alizarin red-S (AR-S) stain. Colorimetric quantification at 510 nm of Alizarin red-S stain was used for quantification of mineralized nodules.

RNA interference assay

RNA interference was used to downregulate the expression of CBS and CSE in hSCs. Gene silencing was achieved by transfecting hSCs with control, nontargeting siRNA (NT siRNA, ON-TARGETplus, nontargeting pool), CTH siRNA (ON-TARGETplus SMARTpool siRNA J-003481), and CBS siRNA (ON-TARGETplus SMARTpool siRNA J-008617) with a pool of four sequences to ensure high-level silencing purchased from Dharmacon (ThermoScientific, Waltham, MA, USA) and INTERFERin, the siRNA transfection reagent (Polyplus Transfection, Illkirch, France, 409-10). Target sequences were as follows: CBS: AGACGGAGCAGACAACCUA, CAGGACGGUGGUGGACAA, GUGCGGAACUACAUGACCA, GGAAGAAGUUCGGCCUGAA; CTH: GUACAGGGAUGGUCACCUU, GCACUCGGGUUUUGAAUAU, CUACAUGUCCGAAUGGAAA, GAGCUUGGGAGGAUUCGAA. Each transfection was performed according to manufacturer instructions and using 20 nM siRNA and 6 μL INTERFERin. The first transfection was performed in hSCs reaching 60% confluence in α-MEM 15% FBS. Afterward, cells were induced with osteogenic medium. Transfection was repeated at every medium change until mineralization was observed in control cells.

Immunohistochemical analysis for CBS and CSE

Tibial plateau biopsies, obtained from male osteoarthritic patients undergoing surgical knee replacement, were fixed, decalcified, dehydrated, embedded in paraffin, and sectioned in 3- to 4-μm-thick slices. Immunostainings were performed on deparaffinized and rehydrated slices for CBS (A01, Abnova, Taipei City, Taiwan) and CSE (M02, Abnova), as well as negative and isotype-matched controls. Positive staining was revealed with Universal AP Detection kit (Biocare Medical, Concord, CA, USA). Specimens were then counterstained with hematoxylin and mounted in glycerol gel. Pictures at ×200 or ×400 magnification were captured by NIS software (Nikon, Firenze, Italy).

μCT measurements

μCT scanning and analysis was performed as reported previously[37,38] using a Scanco μCT-40 in vitro scanner and a Scanco vivaCT-40 for in vivo measurements of spinal trabecular bone (Scanco Medical, Bassersdorf, Switzerland). Voxel sizes were 8 μm^3 and 10.5 μm for the in vitro and in vivo measurements, respectively. For the femoral trabecular region, we analyzed 140 slices from the 50 slices under the distal growth plate. Femoral cortical bone was assessed using 80 continuous CT slides located at the femoral midshaft. For in vivo measurements of spinal trabecular bone, contours along the periosteal surfaces were drawn encompassing 50 slices of the L_1 vertebra, starting at the beginning of trabecular bone within the spinal body, as described.[39] X-ray tube potential was 70 kVp, and integration time was 350 ms for the in vivo measurements and 200 ms for the in vitro measurements.

Quantitative bone histomorphometry

Mice were injected subcutaneously with calcein (25 μg/g) 10 and 3 days before death. Vertebras and femurs were fixed in 10% neutral-buffered formalin for 48 hours, dehydrated and defattened at 4°C, and embedded in methyl methacrylate resin. Nonconsecutive 5-mm longitudinal sections were cut using a Leica RM2155 (Leica Microsystems, Buffalo Grove, IL, USA), stained with Goldner's trichrome stain and used for analysis of static indices. Additional sections were cut at 10 μm and left unstained for dynamic (fluorescent) measurements. Longitudinal sections of L_4 were obtained in the frontal midbody plane. In the femurs, measurements were obtained in an area of cancellous bone that measured ~2.5 mm^2 and contained only secondary spongiosa, which was located 0.5 to 2.5 mm proximal to the epiphyseal growth cartilage of the femurs. Measurements of single-labeled and double-labeled fluorescent surfaces and interlabel width were made in the same region of interest using unstained sections. Mineral apposition rate (MAR) and bone formation rate (BFR/BS) were calculated by the software by applying the interlabel period.

Histomorphometry was performed using the Bioquant Image Analysis System (R&M Biometrics, Nashville, TN, USA). Measurements, terminology, and units used for histomorphometric analysis were those recommended by the Nomenclature Committee of the American Society of Bone and Mineral Research.[40]

H_2S measurement

H_2S and bound sulfur levels were measured in the serum according to previously described methods.[41] For the measurement of H_2S and bound sulfur in serum, 0.1 mL of serum was used for each measurement. The concentrations of H_2S in the samples were calculated using a standard curve of Na_2S as a source of H_2S. Chromatographs were captured and analyzed with Agilent ChemStation software (B.04.03; Agilent Technologies, Santa Clara, CA, USA). For serum, the amount of H_2S is reported as μM.

Murine SCs purification

BM cells were collected at death and BM murine stromal cells (SCs) were purified as previously described.[42,43] Briefly, BM was cultured for 7 days in α-MEM medium containing 10% FBS to allow the proliferation of SCs. After discarding nonadherent cells,

adherent macrophages were eliminated by positive immunoselection by MACS Microbeads (Miltenyi Biotec, Auburn, CA, USA) coupled to anti-CD11c antibody. This marker is expressed on nonadherent dendritic cells and adherent monocytes and macrophages. The remaining adherent cells were defined as SCs because they express ALP, type-I collagen (COLI), and RUNX2, and have the capacity to form mineralization nodules when further cultured under mineralizing conditions.

CFU-ALP assays

Colony-forming assays were carried out according to our previously published protocol. Briefly, colony-forming assays were carried out to determine the number of BM SCs with osteogenic potential, as previously described.[42] Briefly, BM SCs were cultured in α-MEM medium containing 10 mM β-glycerophosphate and 50 μg/mL ascorbic acid at a density of 2×10^6 cells/cm^2. After 7 days, the cells were fixed and stained for ALP and the number of colonies positive for ALP was counted.

Markers of bone turnover

Serum C-terminal telopeptide of collagen (CTX) was measured by a rodent-specific ELISA assay (Immunodiagnostic Systems, Scottsdale, AZ, USA). Serum P1NP was measured using Rat/Mouse P1NP ELISA kit (Immunodiagnostic Systems).

Real-time RT-PCR and PCR arrays

mRNA expression in mice whole BM lysates was analyzed for a cluster of pathway-focused Wnt signaling–related genes by means of PCR Array (Mouse Wnt Signaling Pathway Kit, Qiagen, Milan, Italy), according to the manufacturer's instructions. Briefly, total cellular RNA was isolated using the RNeasy Mini Kit (Qiagen) and contamination of genomic DNA was removed from total RNA samples by treating them with DNase I (DNA-Free Kit, Ambion, Austin, TX, USA). Complementary DNA (cDNA) synthesis was performed from 0.8 αg RNA using the RT2 PCR array First Strand Kit (Qiagen). Amplification was carried out on a Rotor Gene Thermal Cycler (Corbett Research, Qiagen) equipped with a 100-well rotor under cycling and thermal conditions suggested by the manufacturer.

The data were analyzed using the web-based RT2 PCR array Data Analysis tool provided by the manufacturer. The mRNA expression levels of cystathionine-β synthase (Cbs), cystathionine-γ lyases (Cse), bone sialoprotein (Bsp), collagen 1 (CoL1), osteocalcin (Ocn), osterix (Osx), runt-related transcription factor 2 (Runx2), aryl-hydrocarbon receptor (Ahr), axin2 (Axin2), cysteine-rich protein 61 (Cyr61), naked cuticle 2 homolog (Nkd2), transgelin (Tagln), transforming growth factor beta 3 (Tgfb3), thrombospondin 1 (Thbs1), twist gene homolog 1 (Twist1), Wnt1 inducible signaling pathway protein 1 (Wisp1), T-cell factor (Tef), and lymphoid enhancer factor-1 (Lef-1) were also analyzed in mice BM SCs, by RT-PCR using an ABI Prism 7000 or One Step Plus Sequence Detection System and SYBR GREEN PCR Master Mix (Applied Biosystems, Foster City, CA, USA). Changes in relative gene expression between groups were calculated using the $2^{-\Delta\Delta CT}$ method with normalization to 18S rRNA as previously described. All the primers used were designed by Primer Express Software v2.0 (Applied Biosystems) and validated in previous investigations.[37,42,44,45] The primers used were: 5′-ATTCGAACGTCTGCCCTATCA-3′

(forward) and 5-GTCACCCGTGGTCACCATG-3′ (reverse) for 18s rRNA; 5′-GCTGGGCACACTCTCTCAC-3′ (forward) and 5′-CAGGCCTGGTCTCGTGAT-3′ (reverse) for CBS; 5′-ATAGTCGGCTTCGTTTCCTG-3′ (forward) and 5′-TCGGCAGCAGAGGTAACAAT- 3′ (reverse) for CSE; 5′-CCTGATGAAAGGAGGGAGCA-3′ (forward) and 5′-TGGAATTCAGAATTGCCCGA-3′ (reverse) for BSP; 5′-CCCTACTCAGCCGTCTGTGC-3′ (forward) and 5′-GGGTTCGGGCTGATGTACC-3′ (reverse) for CoL1a; 5′-GCCTTCATGTCCAAGCAGGA-3′ (forward) and 5-GCGCCGGAGTCTGTTCACTA-3′ (reverse) for Ocn; 5′-TGTTAGTAACCTGGCCGGG-3′ (forward) and 5′-CATTGGACTTCCCCCTTCTTG-3′ (reverse) for Osx; 5′-CTGTGGTTACCGTCATGGCC-3′ (forward) and 5-GGAGCTCGGCGGAGTAGTTC-3′ (reverse) for Runx2; 5′-GGGACCTCGGGTGACAATAA-3′ (forward) and 5′-CCTCTGTCCTTTTCCAACCG-3′ (reverse) for Ahr; 5′-CAGTGTGAAGGCCAATGGC-3′ (forward) and 5′-TGGGTTCTCGGAAAATGAGG-3′ (reverse) for Axin-2; 5′-GTGAAGTGCGTCCTTGTGGA-3′ (forward) and 5′-TGCCCTTTTTTAGGCTGCTG-3′ (reverse) for Cyr6; 5′-AATTTCAGTCCAAGCACGCC-3′ (forward) and 5′-CGGGACTCTCTCTCCTCTTGC-3′ (reverse) for Nkd2; 5′-CAGCCCAGACACCGAAGCTA-3′ (forward) and 5′-AGGCTTGGTCGTTTGTGGAC-3′ (reverse) for Tagln; 5′-AGGCTTGGTCGTTTGTGGAC-3′ (forward) and 5′-AGGCTGATTGTGGCCAAGTT-3′ (reverse) for TGFβ-3; 5′-GGACCGGGCTCAACTCTACA-3′ (forward) and 5′-AGCTCCGCGCTCTCCAT-3′ (reverse) for Thbs1; 5′-TCGACTTCCTGTACCAGGTCCT-3′ (forward) and 5′-CCATCTTGGAGTCCAGCTCG-3′ (reverse) for Twist1; 5′-ATGCCTGGCTGTGTACCAGC-3′ (forward) and 5′-CCTGCGAGAGTGAAGTTCGTG-3′ (reverse) for Wsp; 5′-GCTGGGCACACTCTCTCAC-3′ (forward) and 5′-CAGGCCTGGTCTCGTGAT-3′ (reverse) for CBS; 5′-ATAGTCGGCTTCGTTTCCTG-3′ (forward) and 5′-TCGGCAGCAGAGGTAACAAT-3′ (reverse) for CSE; 5′-CAGCTCCCCCATACTGTGAG-3′ (forward) and 5′-TGCTGTCTATATCCGCAGGAA-3′ (reverse) for TCF; 5′-GGGACCTCGGGTGACAATAA-3′ (forward) and 5′-CCTCTGTCCTTTTCCAACCG-3′ (reverse) for Wnt 10b; 5′-GTGAGCGGCTGCTTGTCT-3′ (reverse) and 5′-GGTCCCGAAGTAGGAGAGGA-3′ (forward) for BAX; 5′-TGTAGCTTTGCTCCCCTGAC-3′ (reverse) and 5′-CACAGTGTTGGCAGGGTGT-3′(forward) for Bcl2; 5′-CAGCTCCCCCATACTGTGAG-3′ (forward) and 5′-TGCTGTCTATATCCGCAGGAA-3′ (reverse) for Lef 1; and 5′-GGGACCTCGGGT-GACAATAA-30 (forward) and 5′-CCTCTGT CCTTTTC CAAC CG-3′ (reverse) for Wnt10b.

Levels of human mRNA expression were also analyzed in hSCs for CBS and CSE, according to an established protocol.[25] RNA was extracted with RNApure (Euroclone, Milan, Italy), and purified from DNA with DNA-Free Kit (Ambion), according to the manufacturer's instructions.

Reverse transcription (SuperScript VILO cDNA Synthesis Kit; Invitrogen, Life Technologies, Carlsbad, CA, USA) was performed utilizing 0.5 αg of RNA. Polymerase chain reaction (PCR; SYBR PremixEx Taq, TaKaRa Biomedicals, Tokyo, Japan; LightCycler Instrument, Roche, Mannheim, Germany) was performed on 20 ng cDNA.

Relative quantification of PCR products was obtained with the comparative CT method, comparing to the housekeeping mRNA expression of glyceraldehyde-3 phosphate dehydrogenase (GAPDH). Primer sequences were as follows: 5′-AATGGTGACGCTTGGGAA-3′ (forward) and 5′-TGAGGCGGATCTGTTTGA-3′ (reverse) for CBS; 5′-AAGACGCCTCCTCACAAGGT-3′ (forward) and 5′-TATTCAAAACCCGAGTGCTGG-3′ (reverse) for CSE; and 5′-CGGAGTCAACGGATTTGG-3′ (forward) and 5′-CCTGGAAGATGGTGATGG-3′ (reverse) for GAPDH.

Statistical analysis

All values are expressed as mean ± SEM. Prospective data were analyzed by analysis-of-variance (ANOVA) for repeated measures. Cross-sectional data were analyzed by a two-way ANOVA that included the main effects for animal strain and treatment plus the statistical interaction between animal strain and treatment. When the statistical interaction between animal strain and treatment group was not statistically significant ($p > 0.05$) nor suggestive of an important interaction ($p > 0.10$), p values for the main effects tests were reported. When the statistical interaction was statistically significant or suggestive of an important interaction, then t tests were used to compare the differences between the treatment means for each animal strain, applying the Bonferroni correction for multiple comparisons.

Results

Ovx blunts CSE, CBS expression, and H_2S production

H_2S is enzymatically generated by CBS and CSE[20] and can be revealed as free H_2S or bound sulfur, the stored form of sulfur, which can release free H_2S in physiological conditions.[46] To investigate whether estrogen deficiency affects systemic H_2S levels and its production in bone, 10-week-old female C57BL/6 mice were sham operated or ovx. Four weeks after surgery, mice were euthanized and serum H_2S levels assessed. BM was harvested and cultured for 1 week. SCs were then purified and utilized to assess the levels of CBS and CSE mRNAs. Compared with sham-operated mice, ovx mice had ~65% and ~52% lower levels of serum free H_2S and bound sulfur, respectively (Fig. 1*A, B*). The mRNA expression of CBS and CSE in total BM cells and BM SCs were significantly lower in ovx mice than in sham-operated mice (Fig. 1*C–F*).

Therefore, ovx blunts both the serum levels of H_2S and bound sulfur and the expression levels of CBS and CSE in bone.

Pharmacological replacement of H_2S prevents ovx-induced bone loss by increasing bone formation

To investigate whether H_2S deficiency in ovx mice contributes to bone loss, 10-week-old female C57BL/6 mice were sham operated or ovx and treated with the H_2S-donor GYY (1 mg/mouse/d) or vehicle for 4 weeks starting the day of surgery. Uterus weight was decreased by ovx. GYY treatment did not alter uterus weight, demonstrating that GYY does not exert an estrogen agonistic activity (Supplemental Fig. S1).

Confirming the results of the previous experiment, vehicle-treated ovx mice had lower serum free H_2S and bound sulfur levels than sham-operated mice (Fig. 2*A, B*). Treatment with GYY increased free H_2S levels in sham mice and normalized serum H_2S and bound sulfur levels in ovx mice. As a result, vehicle-treated sham-operated mice and GYY-treated ovx mice had similar H_2S and bound sulfur levels, demonstrating that GYY was able to prevent the sulfur deficiency caused by ovx.

To investigate the effects of GYY treatment on bone volume and structure, cancellous bone was analyzed by micro-computed tomography (μCT) utilizing femurs harvested at death. Representative μCT images of femur trabecular bone from all four groups are shown in Fig. 2*C*. Vehicle-treated ovx mice had lower trabecular bone volume (BV/TV) than vehicle-treated sham-operated mice (Fig. 2*D*). GYY-treated ovx mice had higher BV/TV than vehicle-treated ovx mice. Moreover, GYY-treated ovx mice and vehicle-treated sham-operated mice had similar BV/TV values. These findings demonstrate that GYY completely protects against the loss of BV/TV induced by ovx. Interestingly, GYY-treated sham mice had significantly higher BV/TV than vehicle-treated sham mice. Ovx also induced significant losses of cortical volume (Ct.V) and cortical thickness (Ct.Th) in mice treated with vehicle that were prevented by treatment with GYY (Fig. 2*E, F*). Analysis of indices of trabecular structure revealed that trabecular number (Tb.N), trabecular thickness (Tb.Th), and trabecular space (Tb.Sp) were also differentially affected by ovx in vehicle-treated and GYY-treated mice (Fig. 2*G–I*), further attesting to the bone-sparing activity of GYY.

Unexpectedly, analysis of femoral cancellous bone by histomorphometry revealed that ovx did not alter two indices of bone resorption, the number of OCs per bone surface (N.Oc/BS) and the percentage of bone surfaces covered by OCs (Oc.S/BS) in mice treated with vehicle as well as in those treated with GYY (Fig. 3*A, B*). Analysis of dynamic indices of bone formation revealed that ovx increased mineral apposition rate (MAR) (Fig. 3*C*) but not bone-formation rate (BFR/BS) (Fig. 3*D*) in vehicle-treated mice. Moreover, ovx did not affect the percentage of bone surfaces covered by mineralized surfaces (MS/BS) (Fig. 3*E*). GYY-treated ovx mice had significantly higher MAR and BFR/BS compared with vehicle- and GYY-treated sham-operated mice. However, vehicle-treated and GYY-treated ovx mice had similar MAR and BFR/BS values.

Ovx did not increase two static indices of bone formation, the number of OBs per bone surface (N.Ob/BS) and the percentage of surfaces covered by OBs (Ob.S/BS), in vehicle-treated mice. However, GYY-treated ovx mice had higher N.Ob/BS and Ob.S/BS compared with vehicle-treated ovx mice and vehicle-treated sham-operated mice (Fig. 3*F, G*).

Because of the unexpected finding that ovx did not alter most indices of bone resorption and bone formation, we analyzed vertebral cancellous bone by histomorphometry. We found that ovx increased two indices of bone resorption, N.Oc/BS and Oc.S/BS, in vehicle-treated mice (Fig. 4*A, B*). Treatment with GYY did not affect bone resorption in both sham-operated and ovx mice. In vehicle-treated mice, ovx did not increase MAR (Fig. 4*C*) or BFR/BS (Fig. 4*D*). Similarly, MS/BS did not change between sham and ovx vehicle-treated groups (Fig. 4*E*). However, GYY increased BFR/BS and MS/BS in ovx mice and MAR in both sham-operated and ovx mice. Moreover, ovx increased N.Ob/BS and Ob.S/BS in vehicle-treated

mice (Fig. 4*F, G*). Importantly, mice treated with GYY had higher N.Ob/BS and Ob.S/BS compared with the corresponding vehicle-treated group. These findings suggest that GYY prevents ovx-induced bone loss by increasing bone formation. Confirming this hypothesis, ovx increased the serum levels of N-terminal propeptide of type 1 procollagen (P1NP), a marker of bone formation, in vehicle-treated mice. Treatment with GYY induced a further increase in P1NP in ovx mice (Fig. 4*H*). As a result, GYY-treated ovx mice had higher levels of P1NP than all the other groups of sham-operated and ovx mice. Ovx increased the serum levels of C-terminal telopeptide of type 1 collagen (CTX), a marker of bone resorption in vehicle- and GYY-treated mice (Fig. 4*I*). GYY did not significantly affect the serum levels of CTX in ovx mice.

GYY increases SC commitment to the osteoblastic lineage and differentiation

To investigate the role of GYY treatment on SC differentiation, BM was harvested at the end of the treatment period and cultured for 1 week to assess the formation of alkaline phosphatase (ALP)-positive colony-forming unit fibroblasts (CFU-F), herein defined CFU-ALP, an index of SC commitment to the osteoblastic lineage. CFU-ALP formation was ~1.5-fold higher in vehicle-treated ovx mice compared with vehicle-treated sham mice (Fig. 5*A*). Treatment with GYY further increased the number of CFU-ALP in both sham-operated and ovx mice. Accordingly, GYY-treated ovx mice displayed the highest number of CFU-ALP per plate. Next, we investigated the effects of ovx and GYY treatment on the differentiation of SCs into osteoblasts (OBs) by measuring the mRNA levels of four osteoblastic genes that correlate with SC differentiation into OBs. The analyzed genes are runt-related transcription factor-2 (RUNX2), collagen type-1 (COL-I), osterix (OSX), and osteocalcin (OCN) in purified SCs. Analysis of samples from vehicle-treated mice revealed that ovx increases the expression of each of the four analyzed genes (Fig. 5*B*). Treatment with GYY significantly increased the expression of these genes in sham-operated and ovx mice. Accordingly, GYY-treated ovx mice had the highest mRNA levels of RUNX2, COL-I, OSX, and OCN. Together, these findings demonstrate that GYY treatment increases SC commitment to the osteoblastic lineage and increases osteoblast differentiation.

GYY upregulates Wnt ligands in the BM and increases Wnt signaling in SCs

Because osteoblast differentiation is induced by Wnt activation, we sought to investigate the effects of ovx and GYY treatment on Wnt signaling. Therefore, we harvested SCs from sham-operated and ovx mice treated with vehicle or GYY for 4 weeks starting at surgery and analyzed the mRNA expression of genes specifically upregulated by Wnt signaling. The analyzed genes were: aryl-hydrocarbon receptor (Ahr), axin2, cysteine-rich protein 61 (Cyr61), naked cuticle 2 homolog (Nkd2), transgelin (tagln), transforming growth factor β3 (TGFβ3), thrombospondin 1 (Thbs1), Twist gene homolog 1 (Twist1), Wnt1-inducible signaling pathway protein 1 (Wisp1), T-cell factor (TCF), and lymphoid enhancer factor-1 (Lef-1). These genes were chosen because they are sensitive markers of Wnt activation.[47] Analysis of purified SCs revealed that the levels of mRNA for the 11 tested genes were all increased by ovx compared with sham-operated controls. Moreover, treatment with GYY caused a further increase in the mRNA levels of the 11 measured genes in the ovx group and increased the mRNA expression of 8 genes in the sham-operated group (Fig. 5*C*), suggesting that GYY stimulates bone formation by activating Wnt signaling in osteoblastic cells.

Wnt ligands are produced by bone and hematopoietic cells. To investigate whether increased Wnt signaling is linked to an increased production of Wnt ligands, we analyzed the expression of Wnt ligand genes in whole BM. By using an approach based on PCR Array technology, we analyzed mRNA expression of a cluster of 17 Wnt ligands: Wnt1, Wnt2, Wnt3, Wnt5a, Wnt7a, Wnt 7b, Wnt8b, Wnt9, Wnt10a, Wnt10b, Wnt11, Wnt16, Wnt2b, Wnt3a, Wnt4, Wnt5b, Wnt6, and Wnt8a. Regulatory effects of ovx and GYY were detected for Wnt16, Wnt2b, Wnt6, and Wnt10b (Fig. 6*A–D*). In vehicle-treated mice, ovx decreased the mRNA levels of Wnt10b, whereas it had no effect on Wnt16, Wnt2b, and Wnt6. Moreover, we found GYY treatment to increase the BM mRNA levels of Wnt16, Wnt2b, and Wnt10b in both sham-operated and ovx mice. The mRNA level of Wnt6 was increased by GYY in ovx but not sham mice. The largest changes in the expression of Wnt ligands in response to GYY were noted for Wnt16 and Wnt2b. The levels of these two ligands were in fact found to be higher in GYY-treated ovx mice than in vehicle-treated sham-operated mice.

Treatment with GYY arrest bone loss late after ovx

In mice, ovx induces rapid bone loss for at least 8 weeks. To investigate whether treatment with GYY arrests and/or reverses the bone loss induced by ovx, 10-week-old mice were sham operated or ovx and treated with vehicle or GYY for 4 weeks starting 4 weeks after surgery. In vivo prospective measurements of spinal trabecular BV/TV by μCT revealed that vehicle-treated ovx mice sustained continuous bone loss for the 8 weeks of the experiment (Fig. 7*A*). In ovx mice, treatment with GYY prevented spinal bone loss during the treatment period but did not reverse the bone loss that occurred before initiation of the GYY treatment. In fact, GYY-treated ovx mice had similar BV/TV values at the beginning (week 4) and at the end (week 8) of the treatment period. Moreover, at week 8, BV/TV was ~43% higher in GYY-treated ovx mice than vehicle-treated ovx mice. GYY treatment was also effective in increasing BV/TV in sham-operated mice and in blocking the changes in indices of trabecular structure (Tb.N, Tb.Sp, and Tb.Th) induced by ovx in the spine (Fig. 7*B–D*).

Analysis of femoral trabecular bone by in vitro μCT using samples harvested at the end of the treatment period (8 weeks from surgery) confirmed the efficacy of GYY treatment. In fact, BV/TV was ~47% higher in GYY-treated ovx mice than vehicle-treated ovx mice (Fig. 7*E*), and GYY-treated ovx mice and vehicle-treated sham mice had similar values of BV/TV. Vehicle-treated ovx mice had lower Tb.N and increased Tb.Sp compared with the vehicle-treated sham group (Fig. 7*F, H*). Treatment of ovx mice with GYY reversed the changes in these indices of trabecular structure. In this experiment, neither ovx nor GYY treatment affected Tb.Th (Fig. 7*G*). We also investigated the effect of GYY treatment on cortical bone indices. GYY treatment reversed the loss of Ct.V and Ct.Th induced by ovx, leading to values similar to those of sham-operated mice (Fig. 7*I, J*). Furthermore, GYY treatment induced a significant increase in serum levels of P1NP in both ovx and sham-operated mice, confirming that GYY stimulates bone formation (Fig. 7*K*). On the contrary, GYY did not affect ovx-induced increase in CTX levels (Fig. 7*L*). Together the data show that initiation of GYY treatment late after ovx stimulates bone formation, arresting the loss of trabecular and cortical bone in the spine and reverting, at least in part, femoral bone loss induced by ovx.

At death, SCs were isolated and mRNA levels of RUNX2, OSX, OCN, and COL-1 assessed by RT-PCR. Similar to the previous experiment, ovx significantly upregulated the mRNA levels of each of the osteogenic genes analyzed. GYY treatment further increased the expression levels of RUNX2, OSX, OCN, and COL-1 in ovx mice, a finding confirming that GYY increases osteoblast differentiation (Supplemental Fig. S2).

H_2S induces CBS and CSE expression and stimulates osteogenic differentiation of hSC In an effort to translate findings obtained in mice into human preclinical data, we investigated whether CBS and CSE are expressed in human bone tissue. Immunostaining of human bone biopsies revealed that CSE is predominantly expressed in areas surrounding the BM microvasculature and is only weakly expressed in bone lining cells (Fig. 8*A*, a, b). On the contrary, CBS is broadly expressed in bone lining cells as well as in cells embedded in mineral matrix (Fig. 8*A*, d, e). These findings suggest that H_2S is enzymatically generated in bone and BM. To assess if H_2S stimulates osteogenic differentiation of hSC, we treated hSC with a common H_2S donor, NaHS. This agent dose-dependently stimulated osteogenic differentiation of hSC, as shown by the upregulation of BSP expression (Fig. 8*B*) and significantly induced hSC to produce mineralized nodules (Fig. 8*C*). Next, we investigated whether endogenous H_2S production regulates hSC differentiation into osteoblastic cells. siRNA silencing of CBS and CSE decreased CBS and CSE expression by ~75% compared with nontargeting siRNA-transfected (NT) control (Fig. 8*D*). When subject to osteogenic stimulation, hSC carrying CBS and CSE knock-down showed a dramatic reduction in mineralized nodule formation in vitro (Fig. 8*E*), suggesting that endogenous H_2S is necessary for osteogenic differentiation and mineralization of hSC.

Furthermore, to investigate whether estrogen directly regulates CBS and CSE in human bone cells, we stimulated hSCs with 17-β estradiol. After 24-hour stimulation, 17-β estradiol significantly upregulated CSE and CBS expression (Fig. 8*F, G*), suggesting that the endogenous pathway leading to H_2S production is, at least in part, directly induced by estrogen.

Discussion

We report that ovx in mouse blunts the production of H_2S in the BM SCs and total BM cells by downregulating the key enzymes CBS and CSE. Pharmacological restoration of normal serum levels of H_2S prevents ovx-induced bone loss by enhancing bone formation. We also show that estrogen directly regulates CBS and CSE mRNA levels in human SCs.

H_2S is a ubiquitous molecule implicated in important organ-specific functions such as regulation of vasodilation,[22,48] lipid metabolism in the liver,[49] insulin production,[50] or neuronal excitability.[51] The pathway leading to H_2S generation from cysteine involves the enzymes CBS and CSE.[20] We found ovx to regulate the BM levels of CBS and CSE and to decrease the serum levels of free H_2S and bound sulfur. The difference in serum H_2S levels between sham-operated and ovx mice was similar to the difference found between $CSE^{-/-}$ mice[22] or $CBS^{+/-}$ mice and their respective WT controls,[19] a finding that attests to the potency of sex steroids as regulators of H_2S biosynthesis.

SCs produce H_2S, which stimulates the differentiation of SCs into osteoblasts.[19] Accordingly, pharmacological inhibition of H_2S production or genetic silencing of CBS causes osteopenia,[19] kyphosis, and impaired endochondral bone formation.[52] Moreover, patients affected by homocystinuria, the disorder caused by CBS deficiency, have severe osteoporosis[35] and increased fracture risk.[53,54] These studies demonstrate the relevance of H_2S for skeletal development and bone homeostasis in unperturbed conditions. Our findings are the first to link sex steroid deficiency and the resulting bone loss to suppression of CBS/CSE expression and H_2S production. Specifically, we found that in the ovx mouse, a model of postmenopausal osteoporosis, decreased production of H_2S prevents bone formation to increase sufficiently to compensate for increased bone resorption, leading to unbalanced remodeling and net bone loss. Our findings are consistent with earlier reports, which disclosed that loss of estrogens or androgens accelerates the effects of aging on bone by decreasing defense against oxidative stress.[17,55] H_2S levels decrease with aging,[29] and H_2S prevents oxidative stress,[56] suggesting that decreased production of H_2S may mediate or intensify the effects of oxidative stress in bone and account for the effects of both aging and estrogen deficiency in bone.

GYY is a slow-releasing H_2S donor that has been widely used to investigate the role of H_2S in biological processes.[57–59] GYY did not cause an increase in uterus weight, indicating that this agent is devoid of estrogen agonist activity. In this study, we used GYY treatment to prevent ovx-induced bone loss by starting the GYY treatment at the time of surgery. In this experiment, GYY prevented femoral trabecular and cortical bone loss by increasing bone formation. Interestingly, GYY-treated ovx mice had similar trabecular and cortical volume than vehicle-treated sham-operated mice. However GYY-treated sham-operated mice had even higher bone volume than GYY-treated ovx mice and the highest levels of free H_2S, presumably because of the cumulative effects of estrogen and GYY on H_2S synthesis. The existence of a relationship between H_2S levels and bone volume suggest that it may be possible to increase bone volume above baseline and achieve a net bone anabolic effect by treating ovx mice with doses of GYY higher than the dose used in the current study.

In vivo prospective μCT measurements of spinal trabecular bone showed that this agent was not capable of reversing bone loss in this compartment when the treatment was started 4 weeks after surgery. In vivo μCT measurements were not feasible in the femur with our μCT scanner. Therefore, we were unable to assess the effect of GYY in the femur in a prospective fashion. Measurements of femoral bone were obtained in samples harvested at death. This cross-sectional analysis revealed that GYY-treated ovx mice had trabecular and cortical bone volume values higher than those of vehicle-treated ovx mice and similar to those of vehicle-treated sham-operated mice. Although these data suggest a reversal effect, we are unable to conclusively ascertain whether GYY reverses femoral bone loss because of the lack of baseline measurements of bone volume.

The loss of trabecular bone induced by sex steroid deficiency is attributable to a stimulation of bone resorption and is mitigated by a concomitant increase in bone formation. We measured histomorphometric indices of bone turnover in femurs and vertebras harvested at the end of the prevention study. Analysis of femoral samples did not show the expected increase in bone resorption induced by ovx. BFR, BS/MS, and static indices of bone

formation were also not altered by ovx. The reason why the changes in bone turnover typically induced by ovx were not detected by histomorphometric analysis of the femurs is unknown. We hypothesize that these unexpected results are because of the intrinsic low sensitivity and high variability of bone histomorphometry. By contrast, analysis of vertebral samples revealed that ovx increased bone resorption and that GYY treatment did not mitigate the stimulatory effect of ovx on bone resorption. In accordance with the vertebral histomorphometric data, measurements of serum CTX level, which is an accurate marker of bone resorption, revealed that serum CTX was higher in ovx mice than in sham-operated controls, and that GYY treatment did not lower CTX levels. Together, these findings demonstrate that GYY does not prevent bone loss by modulating bone resorption.

Analysis of vertebral indices of bone formation did not show significant changes in MAR, BFR, and BS/MS in response to ovx. However, static indices of bone formation and serum levels of P1NP, which is a sensitive marker of formation, were higher in ovx mice than in sham-operated controls. Importantly, GYY treatment increased all vertebral histomorphometric indices of bone formation and the serum level of P1NP in ovx mice. Altogether, the data suggest that GYY prevents and arrests bone loss induced by ovx in mice by stimulating bone formation. This interpretation is consistent with the earlier report that H_2S is a potent stimulant of osteoblastogenesis and bone formation.[19]

In agreement with this hypothesis are also the results of the mechanistic studies conducted in this investigation. It is well established that ovx increases the commitment of SCs to the osteoblastic lineage, extends OB life span, and increases the differentiation of SCs into OBs.[13] We found that GYY treatment further potentiates osteoblastogenesis and OB life span induced by ovx. Activation of Wnt signaling in SCs and OBs induces OB proliferation[63] <zaq;2> and differentiation[64,65] and promotes OB survival.[66–68] Accordingly, ovx has been previously shown to activate Wnt signaling in osteoblastic cells.[69] Our data confirm that ovx activates Wnt signaling in SCs and demonstrate that GYY further upregulates Wnt signaling in SCs, leading to increased osteoblastogenesis and increased OB life span. Canonical Wnt signaling is induced by Wnt ligands produced by bone and hematopoietic cells. We analyzed the mRNA levels of Wnt ligands in the BM and found that GYY increases the levels of Wnt16, Wnt6, Wnt2b, and Wnt 10b. Wnt16 was recently shown to prevent cortical bone fragility fractures by inducing canonical and noncanonical Wnt signaling in osteoblast and repressing osteoclastogenesis[70] and is therefore a likely essential mediator of the anabolic activity of GYY in cortical bone. Moreover, Wnt6 regulates SC fate by inducing osteoblastogenesis and inhibiting adipogenesis.[71]

Experiments performed on hSCs extend the significance of in vivo findings in mice and lay the ground for potential therapeutic application in humans. The H_2S donor NaHS induces SC differentiation and increased mineralization in hSC, coherent with the findings reported by Liu and colleagues.[19] Moreover, knocking down the expression of CBS and CSE in SCs is sufficient to markedly inhibit their ability to produce mineralized matrix, according to the in vitro assay that recapitulates in vivo bone-forming capacity of SCs. These findings further support the hypothesis that the transcriptional regulation of CBS and CSE, and the resulting H_2S levels in the BM, is one important mechanism by which the osteogenic commitment of

SCs is regulated in mice and humans. Furthermore, 17-β estradiol was found to upregulate both CBS and CSE in hSCs, supporting the hypothesis that estrogen may directly regulate the main enzymes involved in H_2S biosynthesis. Finally, immunohistochemistry on human bone samples revealed that CBS and CSE are broadly expressed in the bone tissue but with different patterns. Although CBS is widely expressed in bone lining cells, the region that harbors late osteoprogenitor cells and mature osteoblasts,[72] CSE is predominantly expressed in the perivascular area of BM microvasculature, a region that was previously shown to give rise to the earliest bone stem cells.[73]

In summary, our findings show that H_2S and its biosynthetic pathway is implicated in the mechanisms by which estrogen regulates bone formation and that the decline in H_2S levels is involved, at least in part, in the bone-wasting effect of ovx in mice. Furthermore, we provide proof of the principle that a “sulfur replacement” therapy is a conceivable novel therapeutic option for preserving bone mass after menopause. Further investigations are needed to determine whether the biosynthetic pathway of H_2S production may provide novel tools for the diagnosis or the prevention of bone loss after menopause.

Supplementary Material

Refer to Web version on PubMed Central for supplementary material.

Acknowledgments

This study was supported by grants from the National Institutes of Health (DK91780, DK007298, and RR028009) and by grant ‘Ricerca Finalizzata’ from the Italian Ministry of Health (RF PE-2011-02348395). JYL was supported by a grant from the National Institutes of Health (AR061453). LG was supported by a fellowship granted by Spinner 2013.

References

1. Riggs BL, Melton LJ 3rd. Evidence for two distinct syndromes of involutional osteoporosis. Am J Med. 1983; 75(6):899–901. [PubMed: 6650542]
2. Riggs BL, Melton LJ 3rd. Involutional osteoporosis. N Engl J Med. 1986; 314(26):1676–86. [PubMed: 3520321]
3. Johnell O, Kanis JA. An estimate of the worldwide prevalence and disability associated with osteoporotic fractures. Osteoporos Int. 2006; 17(12):1726–33. [PubMed: 16983459]
4. Burge R, Dawson-Hughes B, Solomon DH, Wong JB, King A, Tosteson A. Incidence and economic burden of osteoporosis-related fractures in the United States, 2005–2025. J Bone Miner Res. 2007; 22(3):465–75. [PubMed: 17144789]
5. Lewis JR, Hassan SK, Wenn RT, Moran CG. Mortality and serum urea and electrolytes on admission for hip fracture patients. Injury. 2006; 37(8):698–704. [PubMed: 16815394]
6. Cummings SR, Melton LJ. Epidemiology and outcomes of osteoporotic fractures. Lancet. 2002; 359(9319):1761–7. [PubMed: 12049882]
7. Zaidi M. Skeletal remodeling in health and disease. Nat Med. 2007; 13(7):791–801. [PubMed: 17618270]
8. Weitzmann MN, Pacifici R. Estrogen deficiency and bone loss: an inflammatory tale. J Clin Invest. 2006; 116(5):1186–94. [PubMed: 16670759]
9. Sun L, Peng Y, Sharrow AC, et al. FSH directly regulates bone mass. Cell. 2006; 125(2):247–60. [PubMed: 16630814]
10. Nakamura T, Imai Y, Matsumoto T, et al. Estrogen prevents bone loss via estrogen receptor alpha and induction of Fas ligand in osteoclasts. Cell. 2007; 130(5):811–23. [PubMed: 17803905]

11. Krum SA, Miranda-Carboni GA, Hauschka PV, et al. Estrogen protects bone by inducing Fas ligand in osteoblasts to regulate osteoclast survival. Embo J. 2008; 27(3):535–45. [PubMed: 18219273]
12. Martin-Millan M, Almeida M, Ambrogini E, et al. The estrogen receptor-alpha in osteoclasts mediates the protective effects of estrogens on cancellous but not cortical bone. Mol Endocrinol. 2010; 24(2):323–34. [PubMed: 20053716]
13. Jilka RL, Takahashi K, Munshi M, Williams DC, Roberson PK, Manolagas SC. Loss of estrogen upregulates osteoblastogenesis in the murine bone marrow. Evidence for autonomy from factors released during bone resorption. J Clin invest. 1998; 101(9):1942–50. [PubMed: 9576759]
14. Di Gregorio GB, Yamamoto M, Ali AA, et al. Attenuation of the self-renewal of transit-amplifying osteoblast progenitors in the murine bone marrow by 17 beta-estradiol. J Clin Invest. 2001; 107(7): 803–12. [PubMed: 11285299]
15. Kousteni S, Bellido T, Plotkin LI, et al. Nongenotropic, sex-nonspecific signaling through the estrogen or androgen receptors: dissociation from transcriptional activity. Cell. 2001; 104(5):719–30. [PubMed: 11257226]
16. Kousteni S, Han L, Chen JR, et al. Kinase-mediated regulation of common transcription factors accounts for the bone-protective effects of sex steroids. J Clin Invest. 2003; 111(11):1651–64. [PubMed: 12782668]
17. Almeida M, Han L, Martin-Millan M, et al. Skeletal involution by age-associated oxidative stress and its acceleration by loss of sex steroids. J Biol Chem. 2007; 282(37):27285–97. [PubMed: 17623659]
18. Li L, Rose P, Moore PK. Hydrogen sulfide and cell signaling. Annu Rev Pharmacol Toxicol. 2011; 51:169–87. [PubMed: 21210746]
19. Liu Y, Yang R, Liu X, et al. Hydrogen sulfide maintains mesenchymal stem cell function and bone homeostasis via regulation of Ca(2+) channel sulfhydration. Cell Stem Cell. 2014; 15(1):66–78. [PubMed: 24726192]
20. Vandiver M, Snyder SH. Hydrogen sulfide: a gasotransmitter of clinical relevance. J Mol Med (Berl). 2012; 90(3):255–63. [PubMed: 22314625]
21. Abe K, Kimura H. The possible role of hydrogen sulfide as an endogenous neuromodulator. J Neurosci. 1996; 16(3):1066–71. [PubMed: 8558235]
22. Yang G, Wu L, Jiang B, et al. H2S as a physiologic vasorelaxant: hypertension in mice with deletion of cystathionine gamma-lyase. Science. 2008; 322(5901):587–90. [PubMed: 18948540]
23. Kimura Y, Kimura H. Hydrogen sulfide protects neurons from oxidative stress. FASEB J. 2004; 18(10):1165–7. [PubMed: 15155563]
24. Calvert JW, Jha S, Gundewar S, et al. Hydrogen sulfide mediates cardioprotection through Nrf2 signaling. Circ Res. 2009; 105(4):365–74. [PubMed: 19608979]
25. Gambari L, Lisignoli G, Cattini L, Manferdini C, Facchini A, Grassi F. Sodium hydrosulfide inhibits the differentiation of osteoclast progenitor cells via NRF2-dependent mechanism. Pharmacol Res. 2014; 87:99–112. [PubMed: 24998607]
26. Zanardo RC, Brancaleone V, Distrutti E, Fiorucci S, Cirino G, Wallace JL. Hydrogen sulfide is an endogenous modulator of leukocyte-mediated inflammation. FASEB J. 2006; 20(12):2118–20. [PubMed: 16912151]
27. Mirandola P, Gobbi G, Sponzilli I, et al. Exogenous hydrogen sulfide induces functional inhibition and cell death of cytotoxic lymphocytes subsets. J Cell Physiol. 2007; 213(3):826–33. [PubMed: 17516567]
28. Hine C, Harputlugil E, Zhang Y, et al. Endogenous hydrogen sulfide production is essential for dietary restriction benefits. Cell. 2015; 160(1–2):132–44. [PubMed: 25542313]
29. Chen YH, Yao WZ, Geng B, et al. Endogenous hydrogen sulfide in patients with COPD. Chest. 2005; 128(5):3205–11. [PubMed: 16304263]
30. Jain SK, Bull R, Rains JL, et al. Low levels of hydrogen sulfide in the blood of diabetes patients and streptozotocin-treated rats causes vascular inflammation? Antioxid Redox Signal. 2010; 12(11):1333–7. [PubMed: 20092409]
31. Mani S, Li H, Untereiner A, et al. Decreased endogenous production of hydrogen sulfide accelerates atherosclerosis. Circulation. 2013; 127(25):2523–34. [PubMed: 23704252]

32. Wang K, Ahmad S, Cai M, et al. Dysregulation of hydrogen sulfide producing enzyme cystathionine gamma-lyase contributes to maternal hypertension and placental abnormalities in preeclampsia. Circulation. 2013; 127(25):2514–22. [PubMed: 23704251]
33. Yanfei W, Lin S, Junbao D, Chaoshu T. Impact of L-arginine on hydrogen sulfide/cystathionine-gamma-lyase pathway in rats with high blood flow-induced pulmonary hypertension. Biochem Biophys Res Commun. 2006; 345(2):851–7. [PubMed: 16701554]
34. Robert K, Maurin N, Ledru A, Delabar J, Janel N. Hyperkeratosis in cystathionine beta synthase-deficient mice: an animal model of hyperhomocysteinemia. Anat Rec A Discov Mol Cell Evol Biol. 2004; 280(2):1072–6. [PubMed: 15386278]
35. Mudd SH, Skovby F, Levy HL, et al. The natural history of homocystinuria due to cystathionine beta-synthase deficiency. Am J Hum Genet. 1985; 37(1):1–31. [PubMed: 3872065]
36. Manferdini C, Gabusi E, Grassi F, et al. Evidence of specific characteristics and osteogenic potentiality in bone cells from tibia. J Cell Physiol. 2011; 226(10):2675–82. [PubMed: 21302278]
37. Terauchi M, Li JY, Bedi B, et al. T lymphocytes amplify the anabolic activity of parathyroid hormone through Wnt10b signaling. Cell Metab. 2009; 10(3):229–40. [PubMed: 19723499]
38. Tawfeek H, Bedi B, Li JY, et al. Disruption of PTH Receptor 1 in T cells protects against PTH-induced bone loss. PLoS One. 2010; 5(8):e12290. [PubMed: 20808842]
39. Tower RJ, Campbell GM, Muller M, Gluer CC, Tiwari S. Utilizing time-lapse micro-CT-correlated bisphosphonate binding kinetics and soft tissue-derived input functions to differentiate site-specific changes in bone metabolism in vivo. Bone. 2015; 74:171–81. [PubMed: 25613175]
40. Parfitt AM, Drezner MK, Glorieux FH, et al. Bone histomorphometry: standardization of nomenclature, symbols, and units. Report of the ASBMR Histomorphometry Nomenclature Committee. J Bone Miner Res. 1987; 2(6):595–610. [PubMed: 3455637]
41. Nicholson CK, Lambert JP, Molkentin JD, Sadoshima J, Calvert JW. Thioredoxin 1 is essential for sodium sulfide-mediated cardioprotection in the setting of heart failure. Arterioscler Thromb Vasc Biol. 2013; 33(4):744–51. [PubMed: 23349187]
42. Gao Y, Wu X, Terauchi M, et al. T cells potentiate PTH-induced cortical bone loss through CD40L signaling. Cell Metab. 2008; 8(2):132–45. [PubMed: 18680714]
43. Bedi B, Li JY, Tawfeek H, et al. Silencing of parathyroid hormone (PTH) receptor 1 in T cells blunts the bone anabolic activity of PTH. Proc Natl Acad Sci USA. 2012; 109(12):E725–33. [PubMed: 22393015]
44. Li JY, Tawfeek H, Bedi B, et al. Ovariectomy disregulates osteoblast and osteoclast formation through the T-cell receptor CD40 ligand. Proc Natl Acad Sci USA. 2011; 108(2):768–73. [PubMed: 21187391]
45. Li JY, Walker LD, Tyagi AM, Adams J, Weitzmann MN, Pacifici R. The sclerostin-independent bone anabolic activity of intermittent PTH treatment is mediated by T-cell-produced Wnt10b. J Bone Miner Res. 2014; 29(1):43–54. [PubMed: 24357520]
46. Ishigami M, Hiraki K, Umemura K, Ogasawara Y, Ishii K, Kimura H. A source of hydrogen sulfide and a mechanism of its release in the brain. Antioxid Redox Signal. 2009; 11(2):205–14. [PubMed: 18754702]
47. Jackson A, Vayssiere B, Garcia T, et al. Gene array analysis of Wnt-regulated genes in C3H10T1/2 cells. Bone. 2005; 36(4):585–98. [PubMed: 15777744]
48. Zhao W, Wang R. H(2)S-induced vasorelaxation and underlying cellular and molecular mechanisms. Am J Physiol Heart Circ Physiol. 2002; 283(2):H474–80. [PubMed: 12124191]
49. Namekata K, Enokido Y, Ishii I, Nagai Y, Harada T, Kimura H. Abnormal lipid metabolism in cystathionine beta-synthase-deficient mice, an animal model for hyperhomocysteinemia. J Biol Chem. 2004; 279(51):52961–9. [PubMed: 15466479]
50. Yusuf M, Kwong Huat BT, Hsu A, Whiteman M, Bhatia M, Moore PK. Streptozotocin-induced diabetes in the rat is associated with enhanced tissue hydrogen sulfide biosynthesis. Biochem Biophys Res Commun. 2005; 333(4):1146–52. [PubMed: 15967410]
51. Nagai Y, Tsugane M, Oka J, Kimura H. Hydrogen sulfide induces calcium waves in astrocytes. FASEB J. 2004; 18(3):557–9. [PubMed: 14734631]

52. Robert K, Maurin N, Vayssettes C, Siauve N, Janel N. Cystathionine beta synthase deficiency affects mouse endochondral ossification. Anat Rec A Discov Mol Cell Evol Biol. 2005; 282(1):1–7. [PubMed: 15622513]

53. van Meurs JB, Dhonukshe-Rutten RA, Pluijm SM, et al. Homocysteine levels and the risk of osteoporotic fracture. N Engl J Med. 2004; 350(20):2033–41. [PubMed: 15141041]

54. McLean RR, Jacques PF, Selhub J, et al. Homocysteine as a predictive factor for hip fracture in older persons. N Engl J Med. 2004; 350(20):2042–9. [PubMed: 15141042]

55. Manolagas SC. From estrogen-centric to aging and oxidative stress: a revised perspective of the pathogenesis of osteoporosis. Endocr Rev. 2010; 31(3):266–300. [PubMed: 20051526]

56. Kimura Y, Goto Y, Kimura H. Hydrogen sulfide increases glutathione production and suppresses oxidative stress in mitochondria. Antioxid Redox Signal. 2010; 12(1):1–13. [PubMed: 19852698]

57. Li L, Whiteman M, Guan YY, et al. Characterization of a novel, water-soluble hydrogen sulfide-releasing molecule (GYY4137): new insights into the biology of hydrogen sulfide. Circulation. 2008; 117(18):2351–60. [PubMed: 18443240]

58. Li L, Salto-Tellez M, Tan CH, Whiteman M, Moore PK. GYY4137, a novel hydrogen sulfide-releasing molecule, protects against endotoxic shock in the rat. Free Radic Biol Med. 2009; 47(1): 103–13. [PubMed: 19375498]

59. Liu Z, Han Y, Li L, et al. The hydrogen sulfide donor, GYY4137, exhibits anti-atherosclerotic activity in high fat fed apolipoprotein E(-/-) mice. Br J Pharmacol. 2013; 169(8):1795–809. [PubMed: 23713790]

60. Britton RA, Irwin R, Quach D, et al. Probiotic L. reuteri treatment prevents bone loss in a menopausal ovariectomized mouse model. J Cell Physiol. 2014; 229(11):1822–30. [PubMed: 24677054]

61. Zebaze RM, Ghasem-Zadeh A, Bohte A, et al. Intracortical remodelling and porosity in the distal radius and post-mortem femurs of women: a cross-sectional study. Lancet. 2010; 375(9727):1729–36. [PubMed: 20472174]

62. Holzer G, von Skrbensky G, Holzer LA, Pichl W. Hip fractures and the contribution of cortical versus trabecular bone to femoral neck strength. J Bone Miner Res. 2009; 24(3):468–74. [PubMed: 19016592]

63. Kato M, Patel MS, Levasseur R, et al. Cbfa1-independent decrease in osteoblast proliferation, osteopenia, and persistent embryonic eye vascularization in mice deficient in Lrp5, a Wnt coreceptor. J Cell Biol. 2002; 157(2):303–14. [PubMed: 11956231]

64. Jilka RL. Molecular and cellular mechanisms of the anabolic effect of intermittent PTH. Bone. 2007; 40(6):1434–46. [PubMed: 17517365]

65. Bodine PV, Komm BS. Wnt signaling and osteoblastogenesis. Rev Endocr Metab Disord. 2006; 7(1–2):33–9. [PubMed: 16960757]

66. Almeida M, Han L, Bellido T, Manolagas SC, Kousteni S. Wnt proteins prevent apoptosis of both uncommitted osteoblast progenitors and differentiated osteoblasts by beta-catenin-dependent and -independent signaling cascades involving Src/ERK and phosphatidylinositol 3-kinase/AKT. J Biol Chem. 2005; 280(50):41342–51. [PubMed: 16251184]

67. Tobimatsu T, Kaji H, Sowa H, et al. Parathyroid hormone increases beta-catenin levels through Smad3 in mouse osteoblastic cells. Endocrinology. 2006; 147(5):2583–90. [PubMed: 16484320]

68. Bodine PV, Billiard J, Moran RA, et al. The Wnt antagonist secreted frizzled-related protein-1 controls osteoblast and osteocyte apoptosis. J Cell Biochem. 2005; 96(6):1212–30. [PubMed: 16149051]

69. Li JY, Adams J, Calvi LM, Lane TF, Weitzmann MN, Pacifici R. Ovariectomy expands murine short-term hemopoietic stem cell function through T cell expressed CD40L and Wnt10B. Blood. 2013; 122(14):2346–57. [PubMed: 23954891]

70. Zheng HF, Tobias JH, Duncan E, et al. WNT16 influences bone mineral density, cortical bone thickness, bone strength, and osteoporotic fracture risk. PLoS Genet. 2012; 8(7):e1002745. [PubMed: 22792071]

71. Cawthorn WP, Bree AJ, Yao Y, et al. Wnt6, Wnt10a and Wnt10b inhibit adipogenesis and stimulate osteoblastogenesis through a beta-catenin-dependent mechanism. Bone. 2012; 50(2): 477–89. [PubMed: 21872687]

72. Everts V, Delaisse JM, Korper W, et al. The bone lining cell: its role in cleaning Howship's lacunae and initiating bone formation. J Bone Miner Res. 2002; 17(1):77–90. [PubMed: 11771672]

73. Sacchetti B, Funari A, Michienzi S, et al. Self-renewing osteoprogenitors in bone marrow sinusoids can organize a hematopoietic microenvironment. Cell. 2007; 131(2):324–36. [PubMed: 17956733]

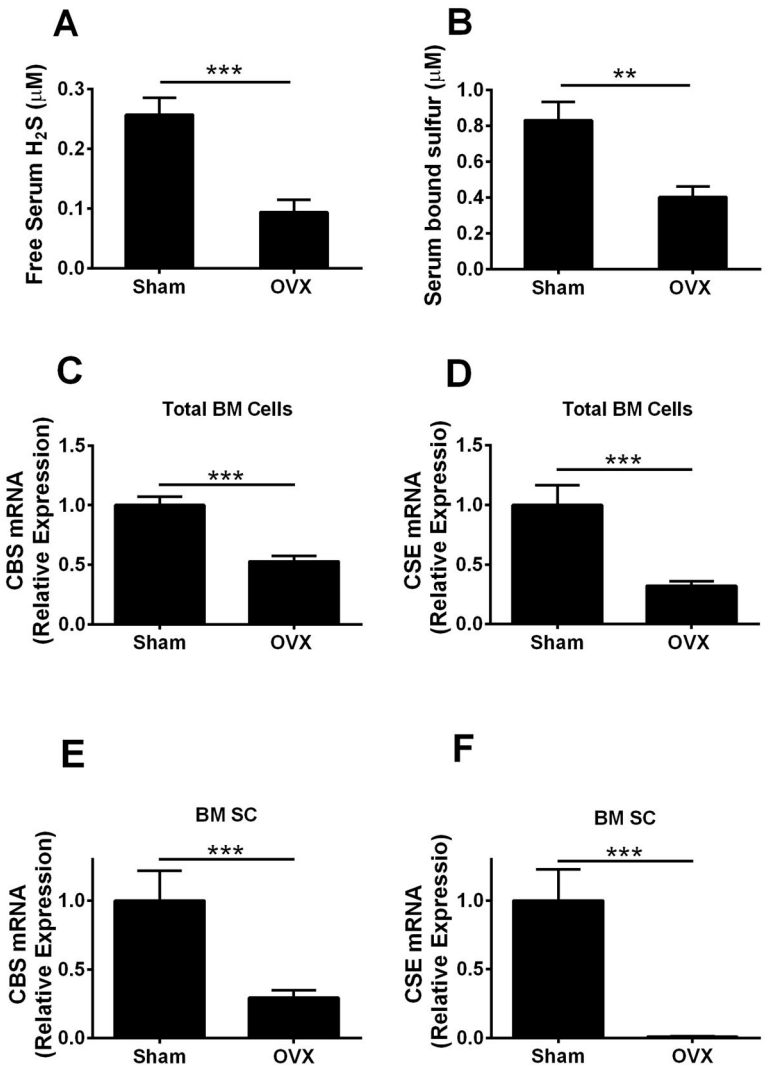

Fig. 1.

Effects (mean ± SEM) of ovx on serum levels of H_2S and mRNA expression of CBS and CSE in BM SCs and total BM cells. (*A*) Serum levels of free H_2S and (*B*) bound sulfur measured 4 weeks after surgery. (*C, D*) mRNA expression of CBS and CSE in total BM cells. (*E, F*) mRNA expression of CBS and CSE in BM SCs. Data are expressed as mean ± SEM. $n = 10$ mice per group. $^{**}p < 0.01$, $^{***}p < 0.001$ compared with the respective sham-operated mice.

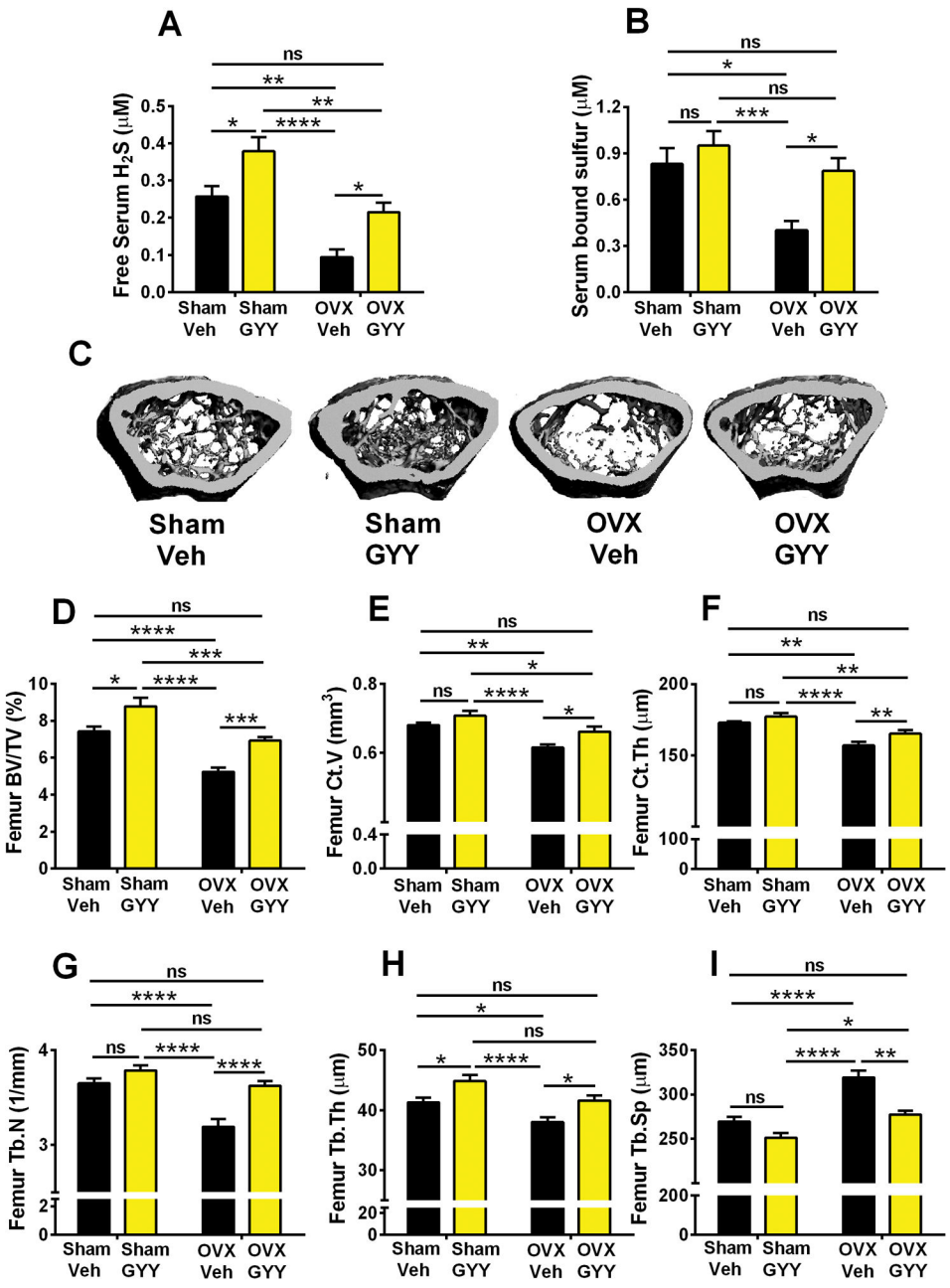

Fig. 2.

Effects (mean ± SEM) of GYY treatment on the serum levels of H_2S and bound sulfur and indices of femoral bone volume and structure as assessed by in vitro μCT scanning. (*A, B*) Serum levels of free H_2S and bound sulfur 4 weeks after surgery. (*C*) 3D image reconstruction of one representative femur per group. (*D*) Trabecular bone volume (BV/TV). (*E*) Cortical bone volume (Ct.V). (*F*) Cortical thickness (Ct.Th). (*G*) Trabecular number (Tb.N). (*H*) Trabecular thickness (Tb.Th). (*I*) Trabecular space (Tb.Sp). $n = 10$ mice per group. *$p < 0.05$, **$p < 0.01$, ***$p < 0.001$, ****$p < 0.0001$ versus the indicated group.

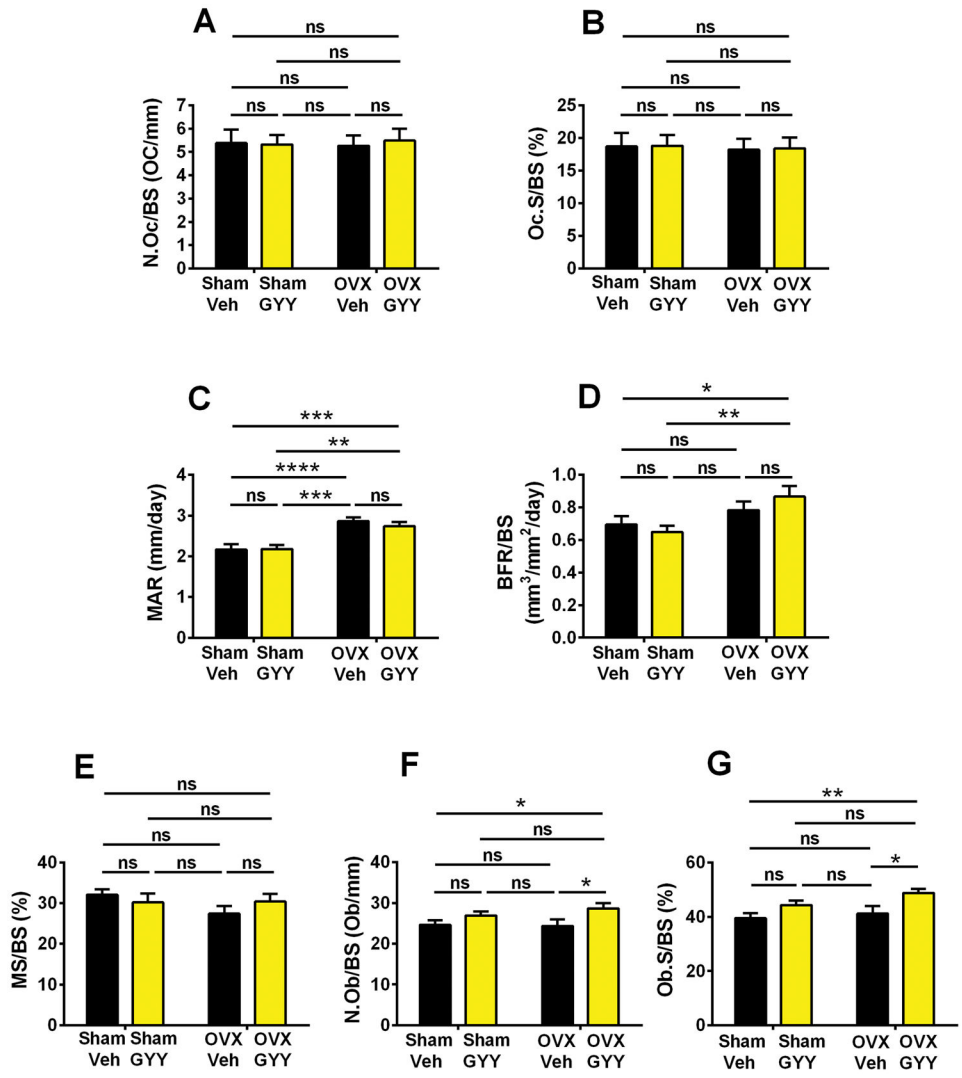

Fig. 3.

Effects (mean ± SEM) of GYY treatment on femoral histomorphometric indices of bone turnover. (*A*) Number of OCs per millimeter of bone surface (N.Oc/BS). (*B*) Percentage of bone surface covered by OCs (Oc.S/BS). (*C*) Mineral apposition rate (MAR). (*D*) Bone formation rate/bone surface (BFR/BS). (*E*) Percentage of bone surfaces covered by mineralized surfaces (MS/BS). (*F*) Number of OBs per bone surface (N.Ob/BS). (*G*) Percentage of bone surfaces covered by OBs (Ob.S/BS). $n = 10$ mice per group. *$p < 0.05$, **$p < 0.01$, ***$p < 0.001$, ****$p < 0.0001$ versus the indicated group.

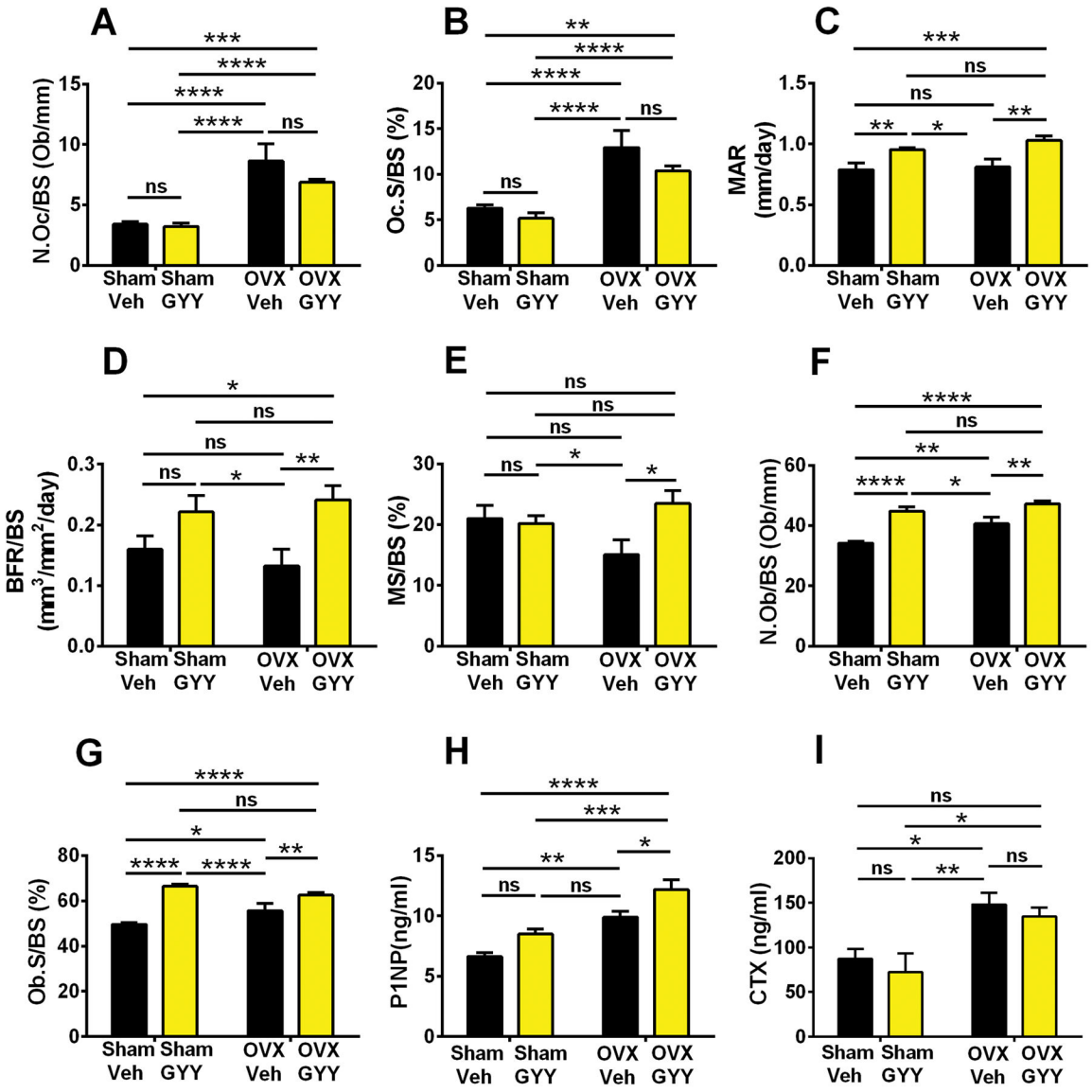

Fig. 4.

Effects (mean ± SEM) of GYY treatment on spinal histomorphometric and biochemical indices of bone turnover. (*A*) Number of OCs per millimeter of bone surface (N.Oc/BS). (*B*) Percentage of bone surface covered by OCs (Oc.S/BS). (*C*) Mineral apposition rate (MAR) and (*D*) bone formation rate/bone surface (BFR/BS). (*E*) Percentage of bone surfaces covered by mineralized surfaces (MS/BS). (*F*) Number of OBs per bone surface (N.Ob/BS). (*G*) Percentage of bone surfaces covered by OBs (Ob.S/BS). (*H*) Serum levels of N-terminal propeptide of type 1 procollagen (P1NP), a marker of bone formation. (*I*) Serum levels of C-terminal telopeptide of type 1 collagen (CTX), a marker of bone resorption. $n = 10$ mice per group. *$p < 0.05$, **$p < 0.01$, ***$p < 0.001$, ****$p < 0.0001$ versus the indicated group.

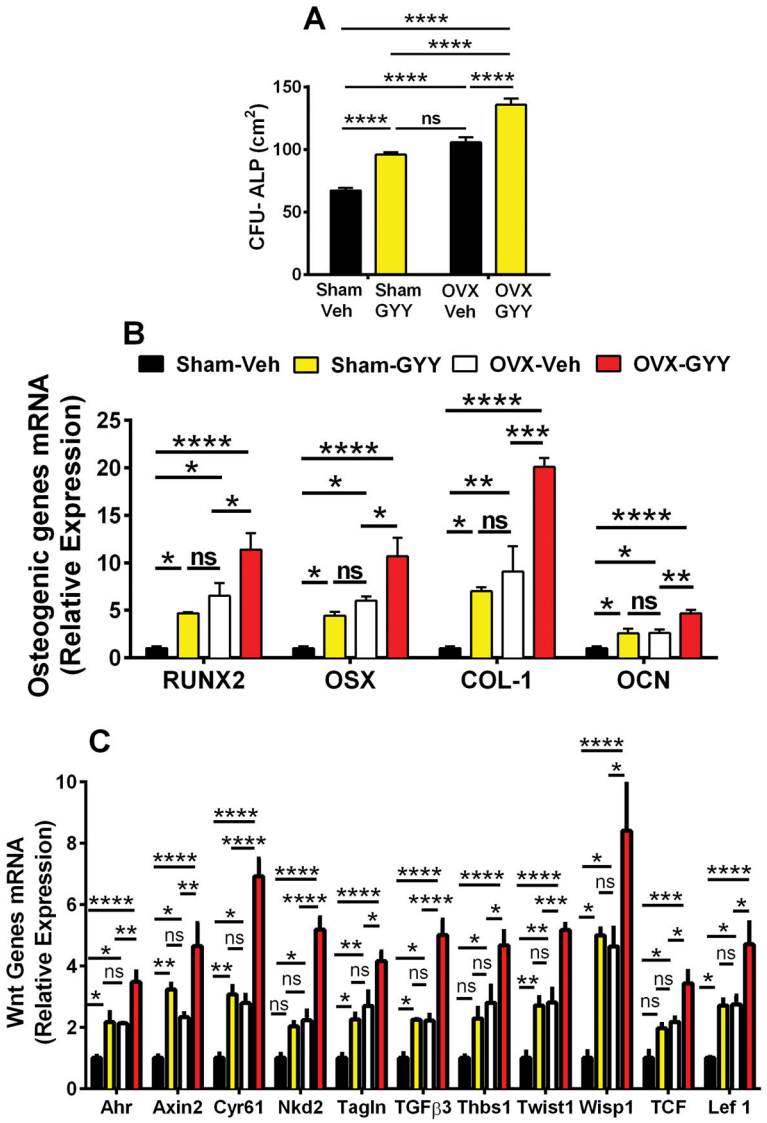

Fig. 5.

Effects (mean ± SEM) of GYY treatment on (*A*) BM CFU-ALP, (*B*) mRNA expression levels of markers of osteogenic differentiation of SCs, and (*C*) SC mRNA expression of Wnt-signaling target genes. $n = 5$ mice per group. *$p < 0.05$, **$p < 0.01$, ***$p < 0.001$, ****$p < 0.0001$ versus sham-operated control.

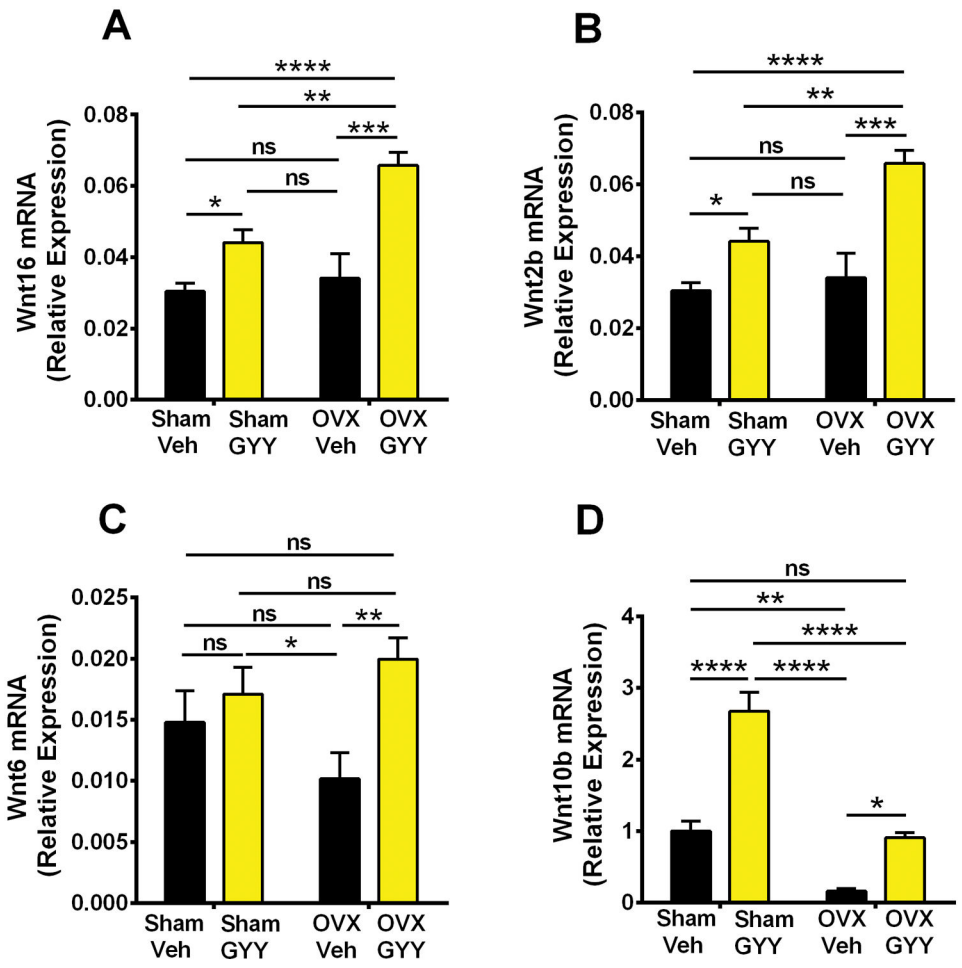

Fig. 6.

Effects (mean ± SEM) of GYY treatment on BM mRNA expression of (*A*) Wnt16, (*B*) Wnt2b, (*C*) Wnt6, and (*D*) Wnt10b. $n = 5$ mice per group. *$p < 0.05$, **$p < 0.01$, ***$p < 0.001$, ****$p < 0.0001$ versus sham-operated control.

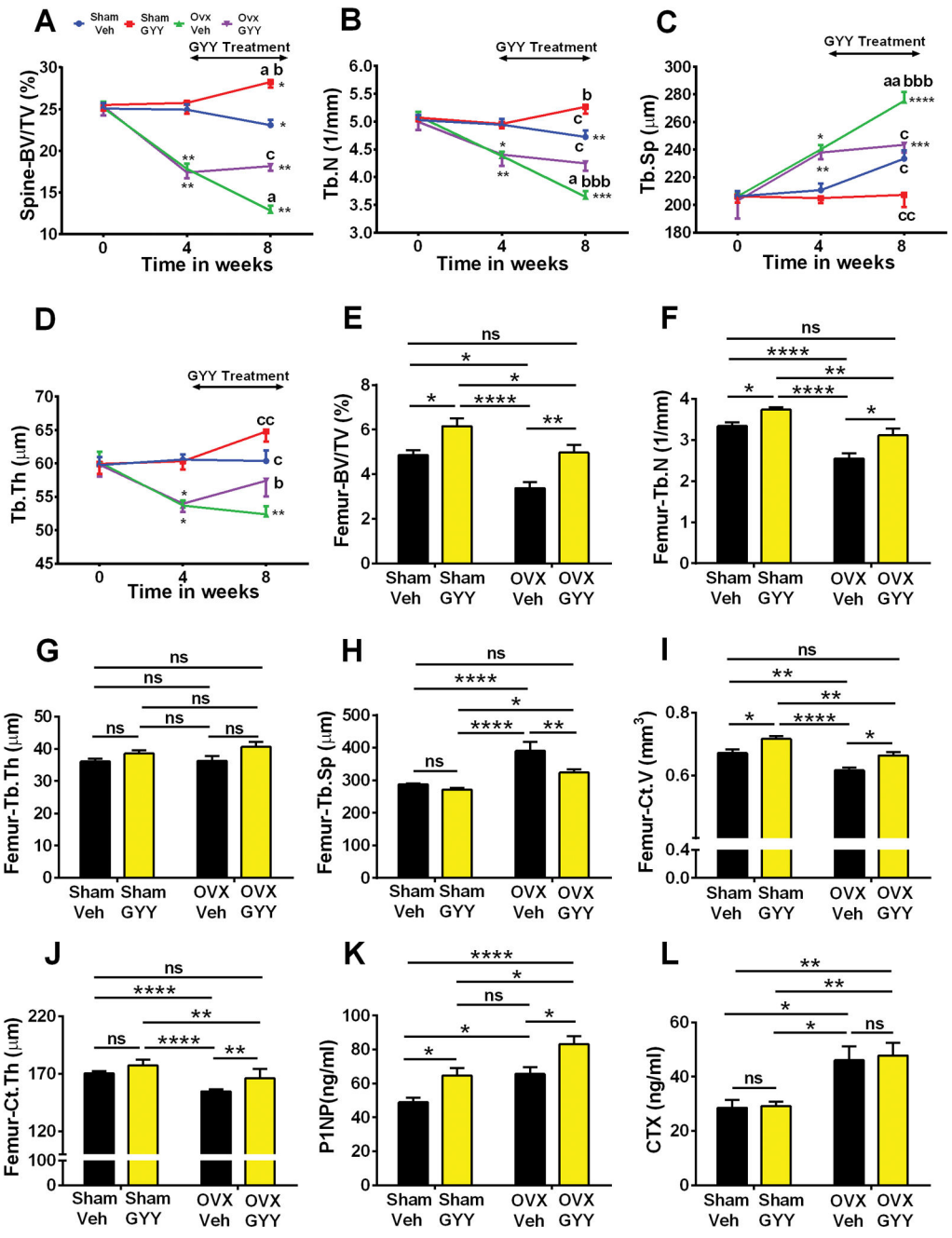

Fig. 7.

Effects (mean ± SEM) of GYY treatment started 4 weeks after ovx or sham operation on spinal bone mass as analyzed by in vivo μCT (*A–D*) and femur bone mass as analyzed by in vitro μCT (*E–J*). (*A*) Spinal bone volume/total volume (BV/TV), (*B*) trabecular number (Tb.N), (*C*) trabecular space (Tb.Sp), and (*D*) trabecular thickness (Tb.Th) as assessed by in vivo μCT scanning. (*E*) Femur bone volume/total volume (BV/TV), (*F*) trabecular number (Tb.N), (*G*) trabecular thickness (Tb.Th), (*H*) trabecular space (Tb.Sp), (*I*) cortical bone volume (Ct.V), and (*J*) cortical thickness (Ct.Th) as assessed by in vitro μCT. (*K*) Serum levels of N-terminal propeptide of type 1 procollagen (P1NP), a marker of bone formation.

(*L*) Serum levels of C-terminal telopeptide of type 1 collagen (CTX), a marker of bone resorption. $n = 10$ mice per group. ****$p < 0.0001$, ***$p < 0.001$. **$p < 0.01$, *$p < 0.05$ versus baseline. a = BL versus week 4; b = versus sham vehicle; c = versus ovx vehicle. a: $p < 0.05$; aa: $p < 0.01$; b: $p < 0.05$; bb: $p < 0.01$; bbb: $p < 0.001$; c: $p < 0.05$; cc: $p < 0.01$.

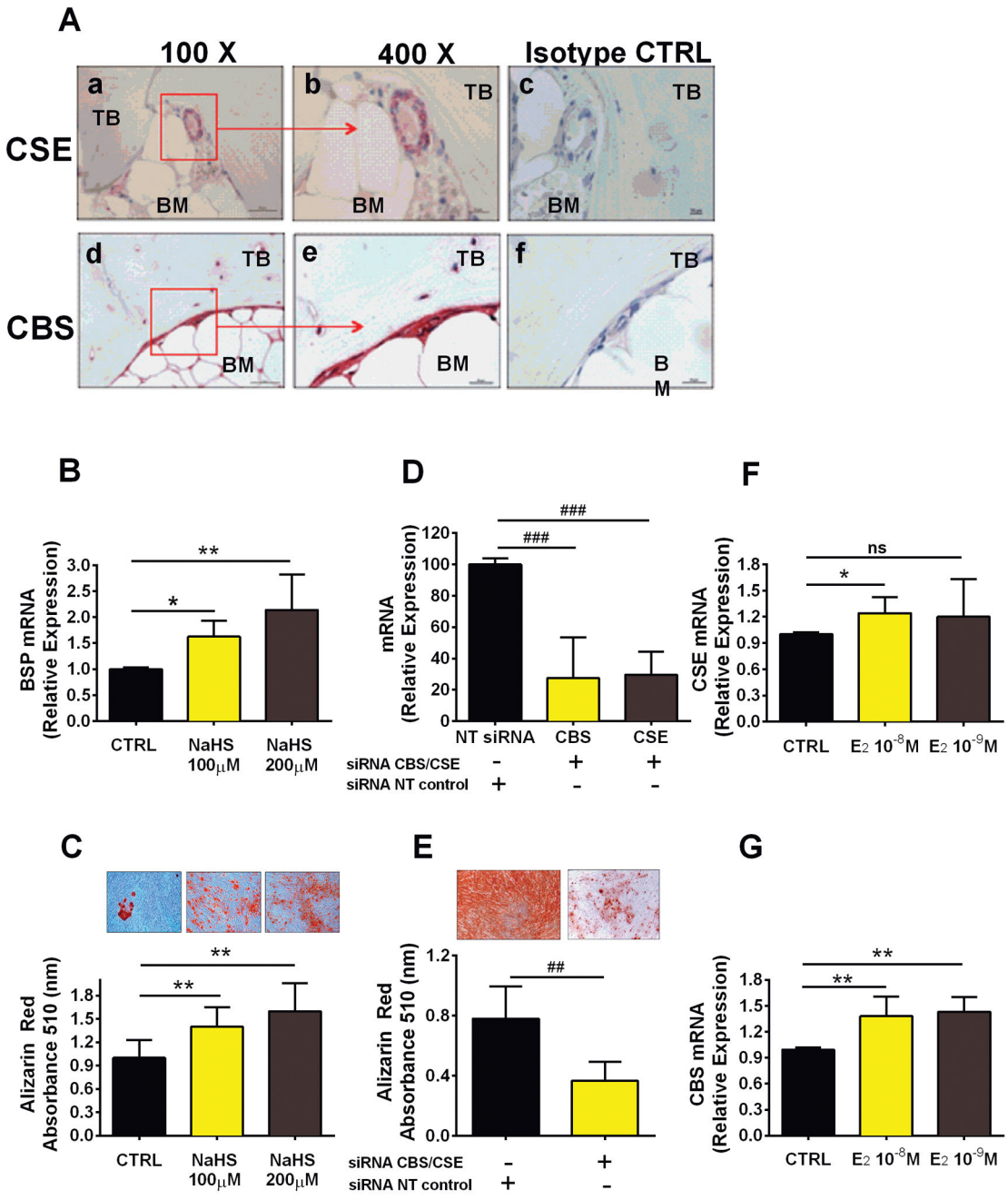

Fig. 8.

H_2S regulates osteogenic differentiation of human BM SCs. (*A*) Immunohistochemistry showing representative pictures of CBS and CSE expression in specimens obtained from human bone biopsies; low-magnification (×100) pictures of (a) CSE and (d) CBS; high-magnification (×400) pictures of (b) CSE and (e) CBS. Isotope control stainings are shown for (c) CSE and (f) CBS. (*B*) Effects of NaHS, an H_2S donor, on mRNA expression of BSP, a common marker of osteogenic differentiation of hSC, and (*C*) the formation of mineralized nodules by hSC under osteogenic stimulation, as evaluated by Alizarin red staining. (*D*) Effect of CBS and CSE knockdown by siRNA on expression levels of CBS and CSE in hSC,

and (*E*) the resulting formation of mineralized nodules by hSC cultured under osteogenic stimulation, as evaluated by Alizarin red staining. Effect of 17β-estradiol (24-hour stimulation) on hSCs mRNA expression of (*F*) CSE and (*G*) CBS. $^{**}p < 0.01$, $^{*}p < 0.05$ versus the respective unstimulated control. $^{\#\#}p < 0.01$, $^{\#\#\#}p < 0.001$ versus the respective nontargeting siRNA (NT) control. Data are expressed as mean ± SEM of results obtained from 5 different donors.